



ELSEVIER

Journal of Chromatography A, 732 (1996) 335–343

JOURNAL OF  
CHROMATOGRAPHY A

## Diffusive analyte loss in capillary electrophoresis caused by delay in field application

Christa L. Colyer, Jan C. Myland, Keith B. Oldham\*

*Department of Chemistry, Trent University, Peterborough, Ont. K9J 7B8, Canada*

Received 14 June 1995; revised 31 October 1995; accepted 21 November 1995

### Abstract

In capillary electrophoresis with sample injection into the capillary mouth, delay between returning the capillary to the inlet reservoir and initiating solution mobilization allows analyte leakage by diffusion from the capillary mouth. This leakage has been modelled on the basis of either convective or diffusive analyte dispersal and the models have been compared with experimental results for peak diminution. Peak widths have also received attention and their utility in estimating analyte amounts has been investigated.

**Keywords:** Diffusion, electrophoresis; Analyte loss; Dispersion; Peak width

### 1. Introduction

In capillary electrophoresis, a standard procedure is to introduce a sample of analyte solution into the front end of the capillary, return the capillary to the reservoir vessel containing running buffer, and immediately turn on the high voltage. The slug of analyte solution, of length  $L$  say, then slowly moves down the capillary column by electroosmosis, arriving at the detector after some time interval  $\Delta t_{\text{transit}}$ , the transit time. During its journey down the capillary, the zone containing the analyte broadens as a result of diffusion (and other, less easily modelled, causes) and ceases to have sharp boundaries [1–6]. Moreover, the maximum concentration diminishes from its original  $c^a$  to a value that can be shown to be

$$c_{\text{peak}} = c^a \operatorname{erf} \left\{ \frac{L}{4\sqrt{D\Delta t_{\text{transit}}}} \right\} \quad (1)$$

where  $\operatorname{erf}\{ \}$  denotes the error function and  $D$  is the diffusivity (diffusion coefficient) of the analyte. For example, using data appropriate to the experimental results presented later in this article, if  $L=2.40 \times 10^{-3}$  m,  $D=9.00 \times 10^{-10}$  m<sup>2</sup> s<sup>-1</sup> and  $\Delta t_{\text{transit}}=405$  s, then  $L/4\sqrt{D\Delta t_{\text{transit}}}=0.994$  and  $c_{\text{peak}}=c^a \operatorname{erf}\{0.994\}=0.840c^a$ . The peak has decayed by about 16%.

Of course there are several other phenomena that may be responsible for loading less (or more) of the analyte onto the column than simple principles suggest. Though some of these effects may lead to corrections of a larger magnitude than the leakage of concern here, they will not be addressed further. Moreover, leakage of any magnitude is not neces-

\*Corresponding author.

sarily detrimental to the purposes of the electrophoretic experiment. Thus, for example, a lengthy delay that is of the same duration in an analytical experiment as in a calibration run may be innocuous.

The previous calculation of a 16% peak diminution assumes that the field is applied immediately after the slug is implanted in the end of the capillary, so that the total amount of analyte in the column remains,  $\pi R^2 L c^a$ , where  $R$  is the radius of the capillary. However, from a variety of causes, deliberate or accidental, there may be a delay of many seconds, or even minutes, before the field is applied and the slug starts its journey. If  $\Delta t_{\text{delay}}$  is the duration of the delay, then the peak will be lower than that predicted by Eq. 1 for two reasons. First, the time interval for the diffusive broadening and peak lowering to have occurred is now longer by  $\Delta t_{\text{delay}}$ . Second, there will be a leak of analyte from the end of the capillary into the reservoir during the interval before the imposition of the field [7]. This document addresses two questions: (a) How much analyte escapes during the delay? and (b) How much lower than predicted by Eq. 1 will the peak now be?

We will investigate two extreme scenarios: when the analyte diffusing from the capillary mouth is dispersed by convection through the buffer solution in the inlet reservoir, and when the dispersal mechanism is by diffusive transport. Experimental results will be compared with prediction (b) for each scenario. Diffusive transport into the capillary can be used as a means of sample injection [7].

A third interesting question, not directly related to the other two, but conveniently answered during our study is (c) how well obeyed is the following "rule of thumb" that is often used to quantify analyte amounts?

(amount of analyte)

$$= (c_{\text{peak}})(\Delta x_{\text{peak}})(\text{cross-sectional area of capillary})$$

(2)

where  $\Delta x_{\text{peak}}$  is the peak width (the length of capillary between the two points at which  $c=1/2c_{\text{peak}}$ ). We can answer this question for the undelayed case by suitably analyzing the equation

$$c = 1/2c^a \operatorname{erf} \left\{ \frac{1/2L - x}{\sqrt{4D\Delta t}} \right\} + 1/2c^a \operatorname{erf} \left\{ \frac{1/2L + x}{\sqrt{4D\Delta t}} \right\} \quad (3)$$

which is presented by Delinger and Davis [4]. This equation describes the shape of the peak formed by diffusive broadening over an interval  $\Delta t$  of a slug of original concentration  $c^a$  and length  $L$ . At  $x = \pm 0.5706L$ , this equation gives  $c=0.420c^a$  when the same values of  $L$ ,  $D$  and  $\Delta t$  are used as previously. This concentration is exactly half of  $c_{\text{peak}}$ , so that  $\Delta x_{\text{peak}}=1.141L$  under these conditions. Hence the product of (peak height) and (peak width) equals  $0.959c^a L$ , indicating that rule (2) underestimates the analyte amount by 4.1% in this case.

## 2. Experimental details and results

All experiments described herein were conducted with an Isco (Lincoln, NE, USA) Model 3850 capillary electropherograph with on-column UV absorbance detection at 190 nm. The high-voltage power supply of this instrument was operated in constant voltage (20.00 kV) mode. The humidity and temperature inside the capillary compartment were not closely controlled, although a fan inside the compartment maintained good ambient circulation. Electropherograms were recorded by a Hewlett-Packard Model HP-7046A x-y chart recorder, and peak transit times, heights and widths were read directly from the chart recordings.

A fused-silica capillary with an external polyimide coating was employed in these studies (Isco). Nominal capillary dimensions were 50  $\mu\text{m}$  I.D., 156.5  $\mu\text{m}$  wall thickness and 16  $\mu\text{m}$  coating thickness, with a measured total length and inlet-to-detector length of 58.3 cm and 33.5 cm, respectively. When not in use, the capillary was filled with distilled, deionized water. One hour prior to daily experimentation, the capillary was refilled with fresh water. The capillary was flushed and filled with running buffer just prior to experimentation, but no flushing between runs was conducted.

A phosphate running buffer, 20.0 mM in each of  $\text{KH}_2\text{PO}_4$  and  $\text{Na}_2\text{HPO}_4$ , was used in these experiments, and was prepared by dissolving reagent grade chemicals (as received, Caledon, Georgetown, Ontario, Canada) in distilled, deionized water. The pH of this buffer, measured by a calibrated Fisher Accumet pH Meter, was found to be 6.84 at 23°C.

Sodium benzoate (NaBz, Caledon) samples were prepared by dissolving sufficient analyte in the phosphate running buffer to produce a 1.00 mM NaBz solution. All solutions were passed through a cellulose acetate syringe filter (pore size 0.45  $\mu\text{m}$ ; Nalge Company, Rochester, NY, USA) and were degassed under vacuum by a water aspirator for approximately 1 h prior to use.

The method of sample injection employed in these studies was split-flow injection [8], which relies on a small fraction of the volume dispensed (5  $\mu\text{l}$  in these experiments) by a microsyringe being deposited into the capillary end, the majority being vented to waste via a short length ( $L_{\text{vent}}=50$  mm) of comparatively wide bore ( $R_{\text{vent}}=90$   $\mu\text{m}$ ) tubing. According to the manufacturer [9], the fraction injected is  $(L_{\text{vent}}/L_{\text{cap}})(R_{\text{cap}}/R_{\text{vent}})^4$ , where  $L_{\text{cap}}$  and  $R_{\text{cap}}$  are the capillary length and radius (583 mm and 25  $\mu\text{m}$  in our experiments). This fraction works out to be  $5.1 \times 10^{-4}$  in our case, so that dispensing a 5.0  $\mu\text{l}$  volume would lead to an injected slug of 2.6 nl volume and 1.3 mm length. However, we are sceptical of this calculation. The formula giving the fraction is based on Poiseuille's Law which assumes that streamlined flow has been achieved, whereas the geometry of the injection port is not conducive to the establishment of a streamlined flow regime. Others [10,11] have found split-flow injection to be a source of inaccuracy and variability. Our experiments suggest that the volume injected in replicate dispensings of 5.0  $\mu\text{l}$  is variable, with the average being about 4.7 nl, rather than the 2.6 nl given by the formula. The 4.7 nl volume is based upon comparing the absorption spectrophotometric response of injected analyte samples with those recorded when the capillary is uniformly filled with analyte of known concentration. An injected volume of 4.7 nl translates to a slug length of  $L=2.4$  mm, which is the figure used in our theoretical calculations.

The results of a large number of experiments, using a variety of delay times are plotted as points in Fig. 1 versus the square root of the delay time. The ordinate is the experimental peak absorbance normalized by the peak absorbance for a two-second delay, this being the minimum feasible with our procedure. The transit times, i.e. the time between switch-on and the arrival of the peak at the detector was effectively constant, in the 400–410 s range.

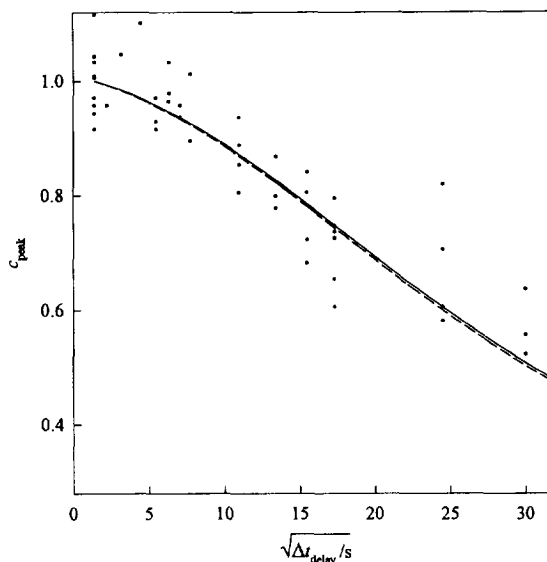


Fig. 1. The points show experimental values of peak height as a function of the delay time  $\Delta t_{\text{delay}}$  between returning the injected capillary mouth into the inlet reservoir and initiating solution motion by applying the electric field. The lines show the results of modelling the same process assuming convective (dashed line) or diffusive (full line) transport of the leaking analyte. In all data, the ordinate values have been normalized by division by the peak height for a 2-s delay.

### 3. Model of leak with convective dispersion

The design of capillary electrophoresis instruments is such that the loading of the sample slug takes place with the capillary mouth out of the inlet buffer reservoir. The capillary mouth must be reimmersed before the field may be applied. Unless measures are taken to prevent it, the act of reimmersion will cause a significant degree of fluid motion in the reservoir, at least temporarily. This convective mixing might be enough to keep the analyte concentration at the mouth of the column effectively zero. In that event, the transport of analyte within the capillary tube obeys Fick's second law

$$\frac{\partial^2 c}{\partial x^2} = \frac{1}{D} \frac{\partial c}{\partial t} \quad (4)$$

subject to the following initial and boundary conditions:

$$c = c^a \quad 0 < x < L, \quad t = 0 \quad (5)$$

$$c = 0 \quad x > L, \quad t = 0 \quad (6)$$

$$c = 0 \quad x = 0, \quad \text{all } t \quad (7)$$

$$c \rightarrow 0 \quad x \rightarrow \infty, \quad \text{all } t \quad (8)$$

Here  $x$  is the axial distance coordinate, measured from an origin at the mouth of the capillary. The solution to this equation set was derived via Laplace transformation [12]. It gives the analyte concentration at any point  $x$  in the capillary as

$$\frac{c}{c^a} = \frac{1}{2} \operatorname{erf} \left\{ \frac{L-x}{2\sqrt{D\Delta t_{\text{delay}}}} \right\} + \operatorname{erf} \left\{ \frac{x}{2\sqrt{D\Delta t_{\text{delay}}}} \right\} - \frac{1}{2} \operatorname{erf} \left\{ \frac{x+L}{2\sqrt{D\Delta t_{\text{delay}}}} \right\} \quad (9)$$

after a delay of  $\Delta t_{\text{delay}}$ . Note that we have treated the analyte concentration as being uniform in each cross-section of the capillary tube. In practice, the nonelectroosmotic flow accompanying injection will create a parabolic front at the junction between the injectant and the preexisting solution. This complication has been ignored.

To answer question (a), we must predict what fraction of the original analyte remains present in the capillary at time  $\Delta t_{\text{delay}}$ . This can be found by comparing the value of the integral

$$n = \pi R^2 \int_0^L c \, dx \quad (10)$$

at the end of the delay period with the original amount (moles) present,  $n_0 = \pi R^2 c^a L$ . One finds

$$\frac{n}{n_0} = \operatorname{erf} \left\{ \frac{L}{2\sqrt{2\Delta t_{\text{delay}}}} \right\} - \frac{2\sqrt{D\Delta t_{\text{delay}}}}{L} \left[ 1 - \exp \left\{ \frac{-L^2}{4D\Delta t_{\text{delay}}} \right\} \right] \quad (11)$$

For the values  $D = 9.0 \times 10^{-10} \text{ m}^2 \text{ s}^{-1}$ ,  $L = 2.40 \times$

$10^{-3} \text{ m}$  and a range of delay times, Eq. 11 predicts the fractional losses reported in Table 1. Notice that a significant percentage of the analyte is lost in the first few seconds, but that over 25 min are required for half the analyte to leak away. For small delay times the formula

$$\frac{n_0 - n}{n_0} \approx \frac{2\sqrt{D\Delta t_{\text{delay}}}}{L} \quad (12)$$

is a good approximation for the fractional loss by convection.

To answer question (b), we need to find the effect of the delay on the peak height. Eq. 9 represents the distribution of analyte at the time the field is switched on. Though it is no longer a “slug”, the analyte travels down the capillary at a constant speed towards the detector. During this journey – which will take virtually the same length of time, the transit time  $\Delta t_{\text{transit}}$ , as before – diffusive broadening occurs and the concentration profile becomes wider and lower. Using Eq. 9 as the starting point, it is not simple to determine the peak concentration  $c_{\text{peak}}$  analytically for any value of the delay time  $\Delta t_{\text{delay}}$ . This prediction of the peak concentration at the detector is, however, easily made via the simulation described in Appendix A. The calculation was

Table 1  
Fraction of analyte leaking from the capillary end, during various delay times, when convection (second column) or diffusion (third column) is the operative dispersal mechanism

$\Delta t_{\text{delay}}/\text{s}$	$1 - (n/n_0)$	
	Convection	Diffusion
0	0	0
1	0.014	0.010
2	0.020	0.014
5	0.032	0.025
10	0.045	0.037
20	0.063	0.055
50	0.100	0.091
100	0.141	0.132
200	0.199	0.190
500	0.314	0.304
1000	0.430	0.420
2000	0.553	0.545
5000	0.697	0.691
$\infty$	1	1

carried out for a series of delay times but for a constant transit time of 405 s. The results are displayed as the broken line in Fig. 1. Note that the only theoretical basis for choosing the square-root of  $\Delta t_{\text{delay}}$ , as the abscissa of this graph comes from the limiting formula (Eq. 12); the choice of the square-root function was made mainly to optimize clarity.

#### 4. Model of leak with diffusive dispersion

In this case, the analyte leaking from the capillary is dispersed diffusively, so that the same transport mechanism applies inside and outside the column. At the mouth of the capillary, diffusion takes the analyte in two directions: further into the capillary, which is innocuous in the sense that this analyte will still eventually reach the detector, and into the reservoir, where it is effectively “lost”.

As in Section 3, we consider diffusion within the capillary, i.e. in zones I and II as illustrated in Fig. 2, to be planar, obeying Fick’s second law in the form of Eq. 4 and meeting all the previous boundary conditions except (Eq.). In the reservoir, however, we treat the diffusion as hemispherical and therefore obeying the alternative form

$$\frac{\partial^2 c}{\partial r^2} + \frac{2}{r} \frac{\partial c}{\partial r} = \frac{1}{D} \frac{\partial c}{\partial t} \quad (13)$$

of Fick’s second law. Here  $r$  is the radial coordinate directed into the reservoir vessel from an origin at the centre of the inlet plane to the capillary. The initial condition

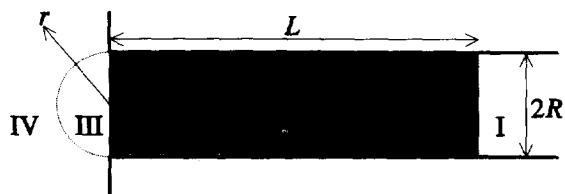


Fig. 2. Diagram, not to scale, showing the geometry of the four zones treated by the model with diffusive dispersion. Only zones I and II are invoked by the model with convective dispersion. The shaded region denotes the initial position of the analyte slug.

$$c = 0 \quad \infty > r > R, t = 0 \quad (14)$$

(recall that  $R$  is the capillary’s inner radius) and the boundary conditions at infinity

$$c \rightarrow 0 \quad r \rightarrow \infty, \text{ all } t \quad (15)$$

apply, as well as two other boundary conditions, numbered (Eq. 16) and (Eq. 17), that will be introduced in the next paragraph. The region  $r > R$ , in which transport is appropriately described by these equations of hemispherical diffusion, will be termed zone IV, as clarified in Fig. 2.

Unfortunately, the planar diffusion in the column and the hemispherical diffusion in the reservoir cannot be matched exactly, and there remains a small region, which we designate zone III, that cannot be ascribed to either region. This has a lenticular shape bounded by the  $r=R$  hemisphere of zone IV and the  $x=0$  end plane of zone II. The volume of this region is very small, which justifies the approximate treatment that is accorded to zone III. This region connects the end of the capillary which is a plane of area  $\pi R^2$ , with the beginning of the region of hemispherical diffusion, which has an area  $2\pi R^2$ . Thus the area changes by a factor of two. Therefore it is reasonable to assume that the concentration halves on proceeding from  $x=0$  to  $r=R$ , so that

$$c_{\text{IV}}(R,t) = c_{\text{III}}(R,t) = 1/2 c_{\text{III}}(0,t) = 1/2 c_{\text{II}}(0,t) \quad (16)$$

In a steady state, the total fluxes across  $x=0$  and  $r=R$  would have the same magnitude and we assume this to be true generally. Since the area doubles, this means that the flux density, and hence the concentration gradient, at  $r=R$  must have half the magnitude of that at  $x=0$ . However, the signs of the two gradients will differ, so that

$$\begin{aligned} \frac{\partial c_{\text{IV}}}{\partial r}(R,t) &= \frac{\partial c_{\text{III}}}{\partial r}(R,t) = -1/2 \frac{\partial c_{\text{III}}}{\partial x}(0,t) \\ &= -1/2 \frac{\partial c_{\text{II}}}{\partial x}(0,t) \end{aligned} \quad (17)$$

Observe that we have ascribed no “diffusive impedance” or other property to zone III. In fact, we shall have no occasion to mention this region again.

The problem is elaborate because of the four zones involved. Nevertheless an exact solution may be obtained by the Laplace transform method [12]. For zone II, the solution, is

$$\begin{aligned} \frac{c_{II}}{c^a} = & 1/2 \exp \left\{ \frac{D\Delta t_{\text{delay}}}{4R^2} + \frac{x}{2R} \right\} \operatorname{erfc} \left\{ \frac{\sqrt{D\Delta t_{\text{delay}}}}{2R} + \frac{x}{2\sqrt{D\Delta t_{\text{delay}}}} \right\} \\ & - 1/2 \exp \left\{ \frac{D\Delta t_{\text{delay}}}{4R^2} + \frac{x+L}{2R} \right\} \operatorname{erfc} \left\{ \frac{\sqrt{D\Delta t_{\text{delay}}}}{2R} + \frac{x+L}{2\sqrt{D\Delta t_{\text{delay}}}} \right\} \\ & + \operatorname{erf} \left\{ \frac{x}{2\sqrt{D\Delta t_{\text{delay}}}} \right\} - 1/2 \operatorname{erf} \left\{ \frac{x+L}{2\sqrt{D\Delta t_{\text{delay}}}} \right\} + 1/2 \operatorname{erf} \left\{ \frac{L-x}{2\sqrt{D\Delta t_{\text{delay}}}} \right\} \end{aligned} \quad (18)$$

where  $\operatorname{erfc}\{\}$  signifies the error function complement,  $1 - \operatorname{erf}\{\}$ . This solution also applies to zone I. Notice that the final three terms, which do not involve the capillary radius, are identical with the three right-hand terms in Eq. 9 for the convective case.

First, we calculate the fraction of the total analyte that is lost. We could find this by a spatial integration of Eq. 18. It is easier, however, to answer question (a) by performing a temporal integration of the flux of analyte across the  $x=0$  plane:

$$\frac{n_0 - n}{n_0} = \frac{D}{c^a L} \int_0^{\Delta t_{\text{delay}}} \frac{\partial c_{II}}{\partial x}(0, t) dt \quad (19)$$

The method used to evaluate this integral again relies on Laplace transformation. The solution may be expressed most concisely in terms of the two dimensionless parameters

$$p = \frac{\sqrt{D\Delta t_{\text{delay}}}}{2R} = \sqrt{\frac{\Delta t_{\text{delay}}}{2.778 \text{ s}}} \quad (20)$$

and

$$q = \frac{L}{2\sqrt{D\Delta t_{\text{delay}}}} = \sqrt{\frac{1600 \text{ s}}{\Delta t_{\text{delay}}}} \quad (21)$$

so that

$$pq = \frac{L}{4R} = 24.00 \quad (22)$$

The numerical values above are based on our standard values  $D=9.0 \times 10^{-10} \text{ m}^2 \text{ s}^{-1}$ ,  $L=2.40 \times 10^{-3} \text{ m}$  and  $R=2.5 \times 10^{-5} \text{ m}$ . In terms of the  $p$  and  $q$  parameters, the integral in Eq. 19 evaluates [12] to

$$\begin{aligned} \frac{n_0 - n}{n_0} = & \frac{1}{q\sqrt{\pi}} [1 - \exp\{-q^2\}] + \frac{4pq + 1}{4pq} \operatorname{erfc}\{q\} \\ & - \frac{1}{4pq} [1 - \exp\{p^2\} \operatorname{erfc}\{p\}] \\ & + \exp\{p^2 + 2pq\} \operatorname{erfc}\{p + q\} \end{aligned} \quad (23)$$

Calculations based on this equation led to the values listed in the final column of Table 1, which presents the fractional analyte loss for a variety of delay times when the loss is due to diffusion from the capillary end. The early values in this column are well approximated by the formula

$$\frac{n_0 - n}{n_0} \approx \frac{2}{L} \left[ \sqrt{\frac{D\Delta t_{\text{delay}}}{\pi}} + \frac{R^2}{\sqrt{D\Delta t_{\text{delay}}}} \right] - \frac{L}{R} \quad (24)$$

Notice that our derivation has neglected the fact that the diffusion process out of and along the capillary is occurring simultaneously with solution flow into and through the capillary. This neglect is only important inasmuch as the flow will perturb somewhat the concentration distribution near the mouth of the capillary, and we believe that such an effect will be minor.

As expected, Table 1 demonstrates a greater effect with convective dispersion than with diffusive dispersion, but the relative difference is small except for short delay times. In practice, one might expect that the paramount dispersion mechanism would be convection initially but that the agitation which gives rise to convective mixing would die down after some seconds, leaving diffusion as the operative mechanism. In any event, errors introduced by the modeling process probably exceed in magnitude the differences between the two sets of results.

Eq. 18, which describes the concentration profile in the capillary at the end of the delay period, must be used to calculate the peak height diminution caused by the delay in applying the field. Once more, we resorted to the simulation method that is explained in Appendix A, using various values of the delay interval  $\Delta t_{\text{delay}}$ . The results are reported as the full line in Fig. 1. As might be expected on the basis of Table 1, there is little difference between the two theoretical lines.

As explained in Appendix A, the simulation was also used to provide data on the peak width, which enabled us to answer question (c). Surprisingly, we found that initially the delay lessens the peak width, presumably because the leak sharpens the initial profile. The peak widths and the peak heights provided by the simulation of the diffusive leak are listed in the second and third columns of Table 2, as normalized equivalents. The fourth column is the

Table 2  
Data to test the “rule of thumb”. (See text for details)

$\Delta t_{\text{delay}}/s$	$\Delta x_{\text{peak}}/L$	$c_{\text{peak}}/c^a$	$(n/n_0)_{\text{Eq. 2}}$	$(n/n_0)_{\text{Tbl}}$	Ratio
0	1.141	0.8401	0.959	1.000	0.959
2	1.133	0.8333	0.944	0.986	0.957
5	1.128	0.8277	0.934	0.975	0.958
10	1.122	0.8205	0.921	0.963	0.956
20	1.117	0.8087	0.903	0.945	0.956
50	1.110	0.7803	0.866	0.909	0.953
100	1.112	0.7414	0.825	0.868	0.950
200	1.133	0.6772	0.767	0.810	0.948
500	1.219	0.5389	0.657	0.696	0.944
1000	1.360	0.4020	0.547	0.580	0.943
2000	1.611	0.2667	0.430	0.455	0.945
5000	2.215	0.1328	0.294	0.309	0.951

product of the two preceding columns and would equal the fraction  $n/n_0$  of analyte in the capillary if the “rule of thumb”, Eq. 2, were obeyed. The correct value of the  $n/n_0$  fraction is available from Table 1 and has been entered into a fifth column of Table 2. Observe that the rule of thumb gives consistently low values, as indicated in the sixth column of the table, which is the quotient of the data in the fourth and fifth columns. This ratio slowly falls from an initial value of 0.959 and reaches a minimum value of 0.943 before again increasing. Observe that the ratio is consistently larger than 0.939, a number whose significance will now be demonstrated.

A gaussian distribution with a standard deviation of  $\sigma$  has a concentration profile described by the equation

$$c(x) = c_{\text{peak}} \exp\left\{-\frac{(x - x_{\text{peak}})^2}{2\sigma^2}\right\} \quad (25)$$

and a total analyte content of

$$n = \pi R^2 \int_{-\infty}^{\infty} c(x) dx = \sqrt{2\pi^3} \sigma R^2 c_{\text{peak}} \quad (26)$$

Any localized distribution will eventually approach such a distribution if planar diffusion is the only dispersive mechanism. At locations a distance  $\sigma\sqrt{\ln\{4\}}$  on either side of the peak, one finds

$$c(x = x_{\text{peak}} \pm \sigma\sqrt{\ln\{4\}}) = c_{\text{peak}} \exp\left\{\frac{\ln\{4\}}{2}\right\} = \frac{c_{\text{peak}}}{2} \quad (27)$$

and therefore the peak width is  $2\sigma\sqrt{\ln\{4\}}$ . Multiplication by  $\pi R^2 c_{\text{peak}}$ , followed by elimination of  $\sigma$  with the help of Eq. 26, leads to

$$\begin{aligned} \pi R^2 c_{\text{peak}} \Delta x_{\text{peak}} &= 2\sigma\sqrt{\ln\{4\}} \pi R^2 c_{\text{peak}} \\ &= 2n\sqrt{\frac{\ln\{4\}}{2\pi}} \end{aligned} \quad (28)$$

From the initial conditions, we know that,  $\pi R^2 c^a L = n_0$  and division of Eq. 28 by that relationship leads to

$$\frac{c_{\text{peak}}}{c^a} \frac{\Delta x_{\text{peak}}}{L} = \frac{2n}{n_0} \sqrt{\frac{\ln\{2\}}{\pi}} = 0.9394 \frac{n}{n_0} \quad (29)$$

Hence, for a gaussian distribution of concentration, the rule of thumb underestimates the quantity of analyte by about 6%. Better ways of estimating the area under gaussian, and other, peaks are discussed by Dyson [13].

## 5. Conclusions

Comparison of the two models shows that convection and diffusion are almost equally effective in fostering a leak of analyte from the mouth of the capillary during the delay prior to electrolyte mobilization in capillary electrophoresis. About 3% of the analyte is lost, under typical conditions, during a 5 s delay and about 10% if 1 m elapses before field application. The corresponding diminutions of peak

height are, however, not proportional to the loss, being 1.5% and 8% respectively in these examples.

We are not proud of the theory/experiment correlation in Fig. 1, the scatter in which we attribute to irreproducibility in the split-flow injector. Nevertheless, there is clear qualitative agreement and no conflict between either model and the experimental results.

The product of peak height and peak width, after peak distortion due to leakage and further delay during electroosmotic transit through the capillary, underestimates the analyte content by 4–6% under the conditions of our experiments. The figure of 6% is appropriate to a gaussian distribution.

### Acknowledgments

We thank the Natural Sciences and Engineering Research Council of Canada, the Trent-Queen's Graduate Program in Chemistry and the Imperial Order of the Daughters of the Empire for financial support.

### Appendix A

A simulation involving a single spatial dimension can provide an answer to the question of how a profile existing within the capillary at  $t=0$  will evolve as it travels down the column, reaching the detector after a time interval  $\Delta t_{\text{transit}}$ . Our prime interest is in what the peak height will be after  $\Delta t_{\text{transit}}$ . Because we are considering only diffusive broadening, our model need not explicitly invoke the motion of the solution down the tube. All that is needed is to transpose the initial profile  $c(x,0)$  into an infinite tube (or, in practice one with  $x$  values ranging from  $-x_{\text{max}}$  through zero to  $x_{\text{max}}$ ) and allow diffusive transport to occur. Simulations with similar goals were carried out by Dose and Guiochon [7].

Our simulation was based on 2000 spatial elements, each corresponding to a length  $\delta x$  of  $1.000 \times 10^{-5}$  m, so that  $x_{\text{max}} = 1.000 \times 10^{-2}$  m. These elements are indexed 0 through 1999 with those indexed 880 through 1119 corresponding to the initial location of the slug,  $0 < x < L$ . The small length element indexed  $j$  corresponds to

$$(j - 1000) \times 10^{-5} \text{ m} < x < (j - 999) \times 10^{-5} \text{ m} \quad (30)$$

The simulation uses 8100 time intervals, each of duration  $\delta t = 0.05000$  s to cover the 405 s of transit time.

To initialize the simulation, each spatial element is accorded a value  $v$  so that the  $j^{\text{th}}$  element has value  $v_j$  equal to the concentration in the centre of the element divided by  $c^a$ . Thus

$$v_{j,0} = \frac{c(x,0)}{c^a} \quad \text{where } x = (j - 879.5) \times 10^{-5} \text{ m} \quad (31)$$

For  $j \leq 879$ , all  $v_{j,0}$  values are zero.

During the simulation, each  $v$  value is updated 8100 times by iteration of the formula

$$v_{j,k+1} = \left[ 1 - \frac{2D\delta t}{(\delta x)^2} \right] v_{j,k} + \frac{D\delta t}{(\delta x)^2} [v_{j-1,k} + v_{j+1,k}] \quad (32)$$

which derives from the discretized version of Fick's second law. There are no exceptions to this formula. With the chosen value  $D = 9.0 \times 10^{-10} \text{ m}^2 \text{ s}^{-1}$  of the analyte's diffusivity, the composite constant  $D\delta t / (\delta x)^2$  has a value of 0.45, which meets the stability criterion of being less than 0.5.

After 8100 iterations the array of  $v$  values is searched to find the element with maximal  $v$  value, which roughly corresponds to the peak concentration at the detector after the transit time has elapsed. A quadratic fit to the  $v$  values of the peak element and those of its two immediate neighbours gives an improved  $v_{\text{peak}}$ . The peak width is found by: (i) identifying the two neighbouring elements, beyond the peak, such that the nearer one has  $v > v_{\text{peak}}/2$  whereas the further one has  $v < v_{\text{peak}}/2$ ; (ii) making a linear interpolation to locate the  $x$  value at which  $v = v_{\text{peak}}$ ; (iii) finding the two adjacent elements before the peak such that  $v_{\text{peak}}$  lies between their  $v$  values; (iv) interpolating to find the exact location of the point at which the concentration is half its peak value; and (v) subtracting the two  $x$  values to find  $\Delta x_{\text{peak}}$ .

Prior to using this simulation to investigate the initial profiles described by Eq. 9 and Eq. 18, we tested the algorithm by using the slug profile given

by Eq. 1. The peak concentration was found to be  $0.8401c^a$ , which is to be identical to the exact value,  $c^a \operatorname{erf}\{L/4\sqrt{Dt}\} = 0.8401c^a$ . Likewise the peak width  $\Delta x_{\text{peak}}$ , measured as 2.741 mm, compared well with the exact value 2.739 mm.

## References

- [1] X. Huang, W.F. Coleman and R.N. Zare, *J. Chromatogr.*, 480 (1989) 95–110.
- [2] F. Foret, M. Deml and P. Boček, *J. Chromatogr.*, 452 (1988) 601–613.
- [3] J.C. Reijenga and E. Kenndler, *J. Chromatogr. A*, 659 (1994) 403–415, 417–426.
- [4] S.L. Delinger and J.M. Davis, *Anal. Chem.*, 64 (1992) 1947–1959.
- [5] A. Vinther and H. Sørensen, *J. Chromatogr.*, 559 (1991) 3–26.
- [6] S. Terabe, O. Shibata and T. Isemura, *J. High Resolut. Chromatogr.*, 14 (1991) 52–55.
- [7] E.V. Dose and G. Guiochon, *Anal. Chem.*, 64 (1992) 123–128.
- [8] J. Tehrani, R. Macomber and L. Day, *J. High Resolut. Chromatogr.* 14 (1991) 10–14.
- [9] ISCO Inc., Model 3850 Electropherograph Instruction Manual, Lincoln NB, 1991, Section 4.2.
- [10] S. Pleasance, P. Thibault and J. Kelly, *J. Chromatogr.* 591 (1992) 325.
- [11] S. Pleasance and P. Thibault, in P. Camilleri (Editor), *Capillary Electrophoresis: Theory and Practice*, CRC Press, Boca Raton, FL, 1993.
- [12] Apply to the authors for details.
- [13] N. Dyson, in R.M. Smith (Series Editor), *Chromatographic Integration Methods*, R.S.C. Chromatography Monographs, Cambridge, 1990.